

EVOLUTION OF CLUSTER X-RAY LUMINOSITIES AND RADII: RESULTS FROM THE 160 SQUARE DEGREE *ROSAT* SURVEY

A. VIKHLININ^{1,5}, B. R. MCNAMARA¹, W. FORMAN¹, C. JONES¹, H. QUINTANA^{2,3}, AND A. HORNSTRUP⁴

ApJ Letters, in press

ABSTRACT

We searched for cluster X-ray luminosity and radius evolution using our sample of 201 galaxy clusters detected in the 160 deg² survey with the *ROSAT* PSPC (Vikhlinin et al. 1998). With such a large area survey, it is possible, for the first time with *ROSAT*, to test the evolution of luminous clusters, $L_x > 3 \times 10^{44}$ ergs s⁻¹ in the 0.5–2 keV band. We detect a factor of 3–4 deficit of such luminous clusters at $z > 0.3$ compared to the present. The evolution is much weaker or absent at modestly lower luminosities, $1\text{--}3 \times 10^{44}$ ergs s⁻¹. At still lower luminosities, we find no evolution from the analysis of the $\log N - \log S$ relation. The results in the two upper L_x bins are in agreement with the *Einstein* EMSS evolution result (Gioia et al. 1990a, Henry et al. 1992) while being obtained using a completely independent cluster sample. The low- L_x results are in agreement with other *ROSAT* surveys (e.g. Rosati et al. 1998, Jones et al. 1998).

We also compare the distribution of core radii of nearby and distant ($z > 0.4$) luminous (with equivalent temperatures 4–7 keV) clusters, and detect no evolution. The ratio of average core radius for $z \sim 0.5$ and $z < 0.1$ clusters is 0.9 ± 0.1 , and the core radius distributions are remarkably similar. A decrease of cluster sizes incompatible with our data is predicted by self-similar evolution models for high- Ω universe.

Subject headings: galaxies: clusters: general — surveys — X-rays: galaxies

1. INTRODUCTION

The cluster evolution rate is a strong test of cosmological parameters (e.g., White & Rees 1978, Kaiser 1986, Eke, Cole & Frenk 1996). It is best to study evolution using X-ray selected samples of distant clusters which are much less affected by projection than the optically selected samples (van Haarlem et al. 1997). Of all the interesting cluster parameters such as mass, velocity dispersion, and temperature, the X-ray luminosity is the most accessible to measurements with present-day instruments, and most of the earlier studies were focused on evolution of the cluster X-ray luminosity function.

A strong evolution of cluster luminosities at $z \sim 0.1$ was reported from the EXOSAT survey (Edge et al. 1990), but was later disproved by the *ROSAT* All-Sky Survey (Ebeling et al. 1997). At higher redshifts, negative evolution of the cluster X-ray luminosity function was first reported by Gioia et al. (1990a) using the *Einstein* Extended Medium Sensitivity Survey (EMSS; Gioia et al. 1990b, Stocke et al. 1991). Gioia et al. and later Henry et al. (1992) compared the cluster luminosity functions below and above $z = 0.3$. They found that while the number of the low luminosity clusters does not evolve, there is a significant deficit of luminous, $L_x(0.3\text{--}3.5\text{ keV}) > 5 \times 10^{44}$ ergs s⁻¹, clusters at high redshift.

This EMSS result was questioned recently. Nichol et al. (1997) reanalyzed the EMSS cluster sample using *ROSAT* X-ray and new optical observations and argued that the evolution reported in the original EMSS papers was not significant. Several groups pursued independent searches for distant clusters in archival *ROSAT* PSPC observations. Collins et al. (1997) found that the redshift distribution of 35 clusters detected in their 17 deg² survey is consistent with no evolution.

This contradicted the earlier claim by Castander et al. (1995) of a strong evolution in a similar sample; however, the latter authors used an X-ray source detection algorithm not optimized for the cluster search. Jones et al. (1998) presented the $\log N - \log S$ relation for 46 clusters from their 16 deg² survey and found that this relation is consistent with no evolution of the $L_x < 2 \times 10^{44}$ ergs s⁻¹ (0.5–2 keV band) clusters. Rosati et al. (1998) derived cluster luminosity functions up to $z \sim 0.8$ from their sample of 70 clusters detected in a 33 deg² survey, and found no evolution at low luminosities, $L_x < 3 \times 10^{44}$ ergs s⁻¹. However, none of these *ROSAT* surveys covers an area large enough to probe the evolution of the luminous clusters, and their no-evolution claims do not contradict the EMSS results.

Our 160 deg² survey (Vikhlinin et al. 1998, hereafter Paper I) is the first *ROSAT* survey comparable with the EMSS in sky coverage for distant clusters. We are able to test, and confirm, the EMSS evolution results even with the incomplete redshift data currently at hand. Eventually, when the spectroscopic work is complete, we will be able to characterize the luminosity evolution more accurately. In this Letter, we also show that the cluster X-ray core radii do not evolve between $z \sim 0.5$ and now. Throughout the paper, we use definitions f_{-14} and L_{44} for flux and luminosity in the 0.5–2 keV energy band in units of 10^{-14} ergs s⁻¹ cm⁻² and 10^{44} ergs s⁻¹, respectively. We also use $H_0 = 50$ km s⁻¹ Mpc⁻¹ and $q_0 = 0.5$.

2. CLUSTER SAMPLE

In Paper I, we presented a catalog of 223 extended X-ray sources detected in 646 high Galactic latitude *ROSAT* PSPC observations. For each detected source, we measured the X-

¹Harvard-Smithsonian Center for Astrophysics, 60 Garden St., Cambridge, MA 02138; avikhlinin@cfa.harvard.edu

²Dpto. de Astronomía y Astrofísica, Pontificia Universidad Católica, Casilla 104, 22 Santiago, Chile

³Presidential Chair in Science

⁴Danish Space Research Institute, Juliane Maries Vej 30, 2100 Copenhagen O, Denmark

⁵Also Space Research Institute, Moscow, Russia

ray flux and angular core-radius. We optically confirmed 89% of detected sources as clusters of galaxies; 8% are false detections due to point source confusion and 3% still lack optical data. In the high X-ray flux range, which is the focus of the present work, 80 out of 82 detected sources are optically confirmed clusters. We measured and compiled from the literature spectroscopic redshifts for 76 clusters. For the rest of the optically confirmed clusters, redshifts are estimated with an accuracy of $\Delta z \approx 0.07$ by optical photometry of the brightest cluster galaxies. All the X-ray and optical data are presented in Paper I. Below we use these data to constrain the evolution of cluster luminosities and sizes at high redshift, $z \sim 0.5$.

TABLE 1

ALL BRIGHT CLUSTERS LACKING SPECTROSCOPIC REDSHIFTS

Name	f_{-14}^a	z^b	z range ^b	z_{\min}^c
2137+0026	27.8	0.05	0.00–0.12	0.5
1301+1059	28.1	0.30	0.23–0.34	0.5
0841+6422	29.1	0.36	0.29–0.40	0.5
1722+4105	29.4	0.33	0.26–0.37	0.5
1641+4001	29.4	0.51	0.44–0.55	0.5 +
1524+0957	30.4	0.11	0.04–0.15	0.5
0259+0013	32.4	0.17	0.10–0.21	0.5
2348–3117	32.5	0.21	0.14–0.28	0.5
0159+0030	32.7	0.26	0.19–0.30	0.5
1515+4346	34.6	0.26	0.19–0.30	0.5
0050–0929	36.6	0.21	0.14–0.25	0.5
2319+1226	38.2	0.25	0.18–0.29	0.5
1146+2854	39.2	0.17	0.10–0.21	0.5
1124+4155	40.1	0.18	0.11–0.22	0.5
0532–4614	41.1	0.10	0.03–0.17	0.5
1013+4933	45.6	0.17	0.10–0.21	0.4
1142+2144	45.9	0.18	0.11–0.22	0.4
0958+5516	48.2	0.20	0.13–0.24	0.4
0237–5224	64.4	0.13	0.06–0.20	0.4
1418+2510	75.6	0.24	0.17–0.28	0.4
1641+8232	80.5	0.26	0.19–0.30	0.3 +
1206–0744	129.0	0.12	0.05–0.16	0.3
1630+2434	179.4	0.09	0.02–0.13	0.3

^a X-ray flux in the 0.5–2 keV band, 10^{-14} ergs s^{-1} cm^{-2} .

^b Photometric redshift and its 95% confidence range.

^c Minimum redshift required for inclusion in the high- L_x , high- z subsample (see text); this redshift is defined by the observed flux. Clusters, whose actual redshifts can possibly exceed this minimum value, are marked +.

3. DEFICIT OF LUMINOUS CLUSTERS AT HIGH REDSHIFT

Cluster evolution is detected in the EMSS sample only for the most luminous clusters, $L_{44} > 5$ in the 0.3–3.5 keV energy band, or $L_{44} \gtrsim 3$ in the 0.5–2 keV band (Gioia et al. 1990a, Henry et al. 1992). The lower-luminosity clusters in the EMSS sample show little or no evolution. We will search for evolution in our sample above this limiting luminosity. Although we cannot derive accurate luminosity functions with the presently incomplete spectroscopic data, a sample of luminous high-redshift clusters can be selected using the observed X-ray flux and the conservative upper bound of their estimated redshift. With such a sample, one can test the evolution of the cluster luminosity function by comparing the number of detected clusters with the prediction of the no evolution model.

3.1. High-Luminosity and High-Redshift Subsample

A luminosity $L_{44} = 3$ corresponds to observed fluxes, $f_{-14} = 77.5$, 44.3, and 27.8 at redshifts $z = 0.3$, 0.4, and 0.5, respectively. Our high-luminosity, high-redshift subsample is defined

using these limiting fluxes as follows. The cluster flux must be $f_{-14} > 77.5$ and redshift must be $z > 0.3$, or $f_{-14} > 44.3$ and $z > 0.4$, or $f_{-14} > 27.8$ and $z > 0.5$. For this sample definition, the lower limit of the luminosity varies with redshift; the variations are, however, limited between $L_{44} = 3$ and 6 for $z < 0.7$.

There are 48 clusters with fluxes $f_{-14} > 27.8$ in our sample. Spectroscopic redshifts are available for 25 of them; none of these 25 clusters satisfies the selection criteria above. The remaining 23 clusters with photometric redshifts are listed in Table 1. Column (4) in this Table shows the 95% confidence interval of the photometric redshift. The observed flux corresponds to the minimum redshift required by our sample definition (column 5). It can be seen that all clusters except 1641+4001 and 1641+8232 can be confidently excluded from the high- L_x , high- z subsample. We conclude that at most, only two clusters belong to this subsample.

3.2. Comparison with No-Evolution Model Predictions

To calculate the expected number of observed clusters, we integrated the local luminosity function (Ebeling et al. 1997) in the appropriate redshift and luminosity range and accounted for the survey solid angle as a function of flux (Paper I). We then compare these predictions with the observed number of clusters in different subsamples. The results are presented in Table 2. For the no-evolution model, we expect 9.3 clusters in the high- L_x , high- z subsample, where we observe at most 2. Such a deviation is significant at more than 99.5% confidence. For the negative evolution observed in the EMSS, we predict that this subsample should contain 2–3 clusters, in agreement with the observed number. Finally, for $q_0 = 0$, the no evolution model predicts 8.1 clusters; the observed deficit is still significant in this case.

For a consistency check, we compare the number of $z < 0.3$ clusters above the same limiting fluxes, $f_{-14} = 77.5$, 44.3, and 27.8, with the prediction of the no evolution model (Table 2); in all flux bins, there is an excellent agreement.

TABLE 2

COMPARISON WITH NO-EVOLUTION MODEL PREDICTIONS

Subsample	Predicted	Observed	Prob
high- L_x , high- z	9.3	2	< 0.005
$z < 0.3$, $f_{-14} > 27.8$	32.5	39	...
$z < 0.3$, $f_{-14} > 44.3$	20.4	21	...
$z < 0.3$, $f_{-14} > 77.5$	11.3	10	...
$z > 0.4$, $f_{-14} > 13.9$	22.2	18	0.22

We also can compare the observed and predicted number of lower-luminosity clusters at high redshift. For that, we use a subsample of clusters with fluxes in the range $13.9 < f_{-14} < 44.3$ and $z > 0.4$. This flux range at $z = 0.4$ corresponds to the luminosity range $1 < L_{44} < 3$, which combines the two lowest luminosity bins in the EMSS luminosity function at high redshift. To obtain a conservative lower limit of the number of observed clusters, we use the lower bound of photometric redshifts. We find 18 clusters, compared with 22.2 predicted by the no-evolution model. That is, the evolution in this interval is certainly different from that of the high L_x clusters.

To summarize, we find a large deficit, by a factor of 3–4, of $L_{44} > 3$ clusters at high redshift, similarly to the EMSS result.

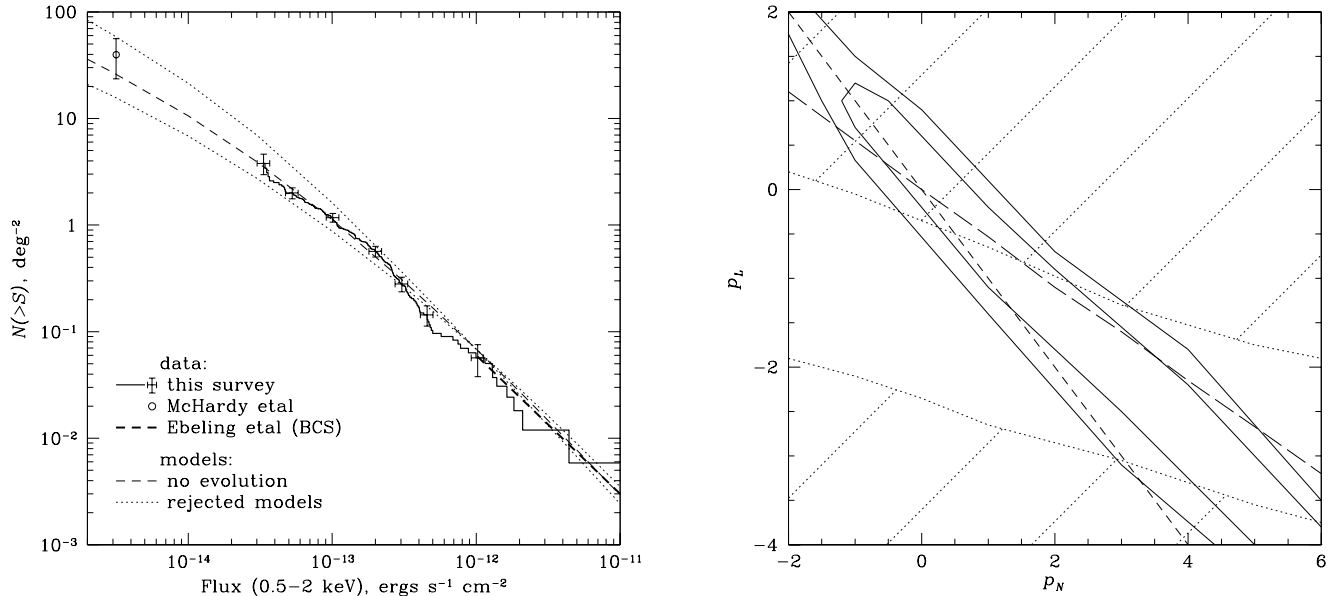


FIG. 1.— Fit to the $\log N - \log S$ relation. The observed $\log N - \log S$ relation (a) was fit by a family of evolution models which combine luminosity and density evolutions as $(1+z)^{p_L}$ and $(1+z)^{p_N}$, respectively. Solid lines in panel b show 68% and 95% confidence intervals of p_N and p_L . The short- and long-dashed lines in (b) correspond to no-evolution of the comoving volume emissivity of clusters at $z = 0.5$, obtained by integration of the luminosity function from 0 to ∞ (short dash) or from 10^{42} to 10^{46} ergs s^{-1} (long dash). Shaded regions in the right panel correspond to parameters which predict either too many (top, > 6.3) or too few (bottom, < 0.36) clusters in the high- L_x , high- z sample. The no-evolution model is shown as a dashed line in (a). All allowed models predict virtually the same $\log N - \log S$. To illustrate the accuracy of the fit, we show two rejected models, $p_N = 0, p_L = -1$ and $p_N = 2, p_L = 0$ (lower and upper dotted lines in the left panel, respectively). Error bars show statistical uncertainties of the measured $\log N - \log S$ at several representative fluxes. Note that the no-evolution model derived by Rosati et al. (1998) differs from that shown here by 10–20% since they integrated only to $z = 1.1$ and used a different local luminosity function.

The evolution rate is smaller at lower luminosities, $1 < L_{44} < 3$, again similar to the EMSS and other *ROSAT* surveys (Rosati et al. 1998). At still lower L_x , our redshift database is very incomplete, but additional constraints on cluster evolution can be derived from the $\log N - \log S$ relation, as described below.

4. LOG N - LOG S RELATION FOR CLUSTERS

The number of clusters as a function of flux (the $\log N - \log S$ relation) can provide some constraints on evolution without redshift information. To obtain the evolution constraints from the $\log N - \log S$, we parameterize the evolution of the luminosity function as a combination of pure luminosity and pure number density evolution, both as powers of $(1+z)$. With this type of evolution, the luminosity function at redshift z can be expressed through the local luminosity function $F_0(L)$ as:

$$F_z(L) = (1+z)^{p_N} F_0(L/(1+z)^{p_L}). \quad (1)$$

In this equation, p_N and p_L parameterize the rate of the density and luminosity evolution, respectively. These parameters can be constrained by fitting the observed $\log N - \log S$ relation.

To predict the model $\log N - \log S$ relation, we integrated the local luminosity function (Ebeling et al. 1997), scaled according to eq. (1) in the redshift interval $0 < z < 2$ and in the luminosity interval $0.01 < L_{44} < 100$. The model $\log N - \log S$ was normalized by the surface density of clusters expected in the no-evolution model above 10^{-12} ergs $s^{-1} \text{ cm}^{-2}$, approximately the completeness limit of the Ebeling et al. *ROSAT* All-Sky Survey sample. Finally, we multiplied the model $\log N - \log S$ relation by the solid angle of our survey as a function of flux (Paper I).

We then found the allowed range of parameters p_N and p_L using the *C*-statistic (Cash 1979) calculated in the flux range

(f_{-14}) from 100 to 4, where the solid angle of our survey still exceeds 4 deg^2 . The 68% and 95% confidence region is shown by solid lines in the right panel of Fig 1. The allowed combination of p_N and p_L corresponds approximately to a non-evolving comoving volume emissivity. The dotted and dashed lines in the right panel correspond to no evolution of the volume emissivity of all clusters (i.e. defined by $p_N + p_L = 0$), and clusters in the range $10^{42} - 10^{46}$ ergs s^{-1} at $z = 0.5$, respectively. The no-evolution model ($p_N = 0, p_L = 0$) is shown by the dashed line in the left panel of Fig 1. All the allowed p_N, p_L parameters predict virtually the same $\log N - \log S$ relations. On the contrary, the rejected models predict $\log N - \log S$ relations which are markedly different from the data (dotted lines in the left panel of Fig 1).

The observed $\log N - \log S$ relation favors no evolution of the cluster volume emissivity. This indirectly implies that the luminosity function at low L_x , which dominates the volume emissivity, does not evolve. This, however, does not imply that there is no evolution at all. For example, the $p_N = 4, p_L = -3$ model is allowed. Since the power-law slope of the luminosity function is close to -1.8 (Ebeling et al. 1997), the number of low luminosity clusters, $L_{44} < 1$, does not evolve in this model, while the number of $L_{44} > 3$ clusters decreases significantly at $z > 0.3$. This behavior is similar to what we find in §3.

5. EVOLUTION OF CLUSTER SIZES

In Paper I, we measured angular core radii by fitting surface brightness distributions with the β -model (e.g., Jones & Forman 1984). Here we compare the radius distribution for our distant, $z > 0.4$, clusters and for nearby clusters in Jones & Forman (1998) sample. To convert angular radii to proper sizes

of distant, $z > 0.3$, clusters, we used both spectroscopic and photometric redshifts. The accuracy of the photometric redshift, ± 0.07 , is sufficient for this purpose. The corresponding proper size uncertainty is 15% at $z = 0.3$, which is smaller than the statistical uncertainty of the angular radius measurements, $\sim 20\%$. Jones & Forman fitted both core-radius and β while we fixed $\beta = 0.67$ for distant clusters. For consistency, we converted core radii from Jones & Forman to $\beta = 0.67$ using Eq. (4) of Paper I. Since Jones & Forman found a correlation between core-radius and luminosity, we matched the luminosity ranges by using only clusters with $1 < L_{44} < 5$ (corresponding to temperatures 4–7 keV) in both samples. The luminosities of distant clusters were computed using both spectroscopic and photometric redshifts. The accuracy of photometric redshifts is sufficient because radius is a weak function of luminosity. The median redshift of the 25 selected distant clusters is $z_{\text{med}} = 0.51$. The uncertainty of an individual radius measurement is $\lesssim 30\%$, which includes photon statistics, background modeling, and scatter in β -parameters (Paper I). This is significantly smaller than the intrinsic width of the derived radius distributions.

The core radius distributions for distant and nearby clusters are remarkably similar (Fig. 2), especially for $q_0 = 0$. To characterize the radius evolution quantitatively, we use the ratio of median radii in both samples. The median radius is 240 ± 14 kpc for nearby clusters, and 210 ± 14 kpc ($q_0 = 0.5$) or 230 ± 16 kpc ($q_0 = 0$) for distant clusters. The ratio lies in the range 0.95–1.25. Some models predict a much stronger evolution of radii. For example, in Kaiser’s (1986) self-similar models, the cluster radius grows by a factor of ~ 2 from $z = 0.4$ to the present, while hydrodynamic simulations with $\Omega + \Lambda = 1$ (Cen & Ostriker 1994) show a factor of 1.5 growth. However, neither these models nor our measurements account for cooling flows (e.g. Fabian 1994) which can cause underestimation of the core-radius. A comparison of core radii is not meaningful if the cooling flow fraction changes with redshift.

6. CONCLUSIONS

We present a first *ROSAT* analysis of the evolution of luminous, $L_x > 3 \times 10^{44}$ ergs s^{-1} distant clusters. We find a significant, factor of 3–4, decrease in the number of such clusters at $z > 0.3$, confirming the detection of evolution in the EMSS (Gioia et al. 1990a, Henry et al. 1992). At lower luminosities, $1\text{--}3 \times 10^{44}$ ergs s^{-1} , the evolution is undetectable, with a decrease in number by a factor of only 1.3 ± 0.2 . This is also consistent with the EMSS and other *ROSAT* surveys (e.g. Rosati et al. 1998). The absence of evolution of low luminosity clusters is also supported by the analysis of the $\log N - \log S$ distribution

from which we find that the cluster volume emissivity, dominated by low-luminosity objects, does not evolve. The observed evolution can be reproduced by a model in which the characteristic luminosity decreases with redshift, but the comoving number density of clusters increases. Such models arise naturally in the hierarchical cluster formation scenario (e.g. Kaiser 1986).

We compare the distribution of core-radii of distant, $z > 0.4$ and nearby clusters. We find that the distribution of core radii at $z > 0.4$ is very similar to that in nearby clusters; the average radius has changed at $z > 0.4$ by a factor of only 0.9 ± 0.1 . A stronger change is expected for hierarchical cluster formation in a flat universe (Kaiser 1986, Cen & Ostriker 1994). We also note that the assumption of no evolution of cluster sizes has been essentially used in flux measurements and area calculations in several X-ray surveys (e.g. EMSS, Nichol et al. 1997), but is only verified here for the first time.

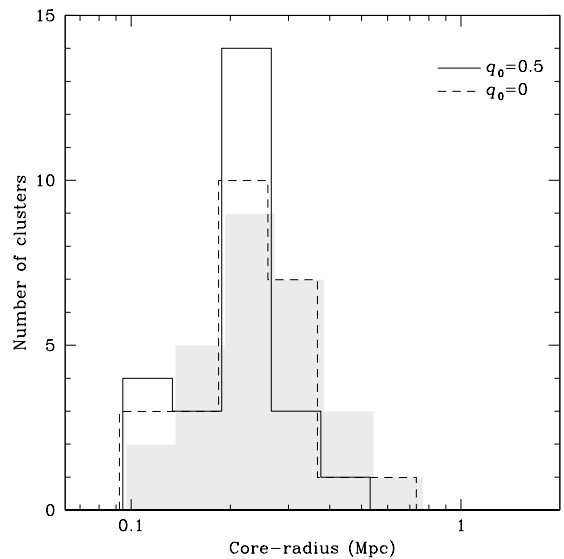


FIG. 2.— Core-radius distribution for distant, $z > 0.4$, clusters, derived from our survey (solid and dashed histogram for $q_0 = 0.5$ and $q_0 = 0$, respectively). The shaded histogram shows the core-radius distribution for nearby luminous clusters from Jones & Forman (1998). The angular resolution limit of our survey ($15''$) corresponds to 120 kpc at the median redshift of distant clusters, well below the peak of the distribution.

We thank M. Markevitch for useful comments on the manuscript. Financial support was provided by the Smithsonian Institution and NAS8-39073 contract. HQ acknowledges support from FONDECYT grant 8970009 and the award of Presidential Chair in Science.

REFERENCES

- Cash, W. 1979, *ApJ*, 228, 939
 Castander, F. J. et al. 1995, *Nature*, 377, 39
 Cen, R. & Ostriker, J. P. 1994, *ApJ*, 429, L4
 Collins, C. A., Burke, D. J., Romer, A. K., Sharples, R. M., & Nichol, R. C. 1997, *ApJ*, 479, L117
 Ebeling, H., Edge, A. C., Fabian, A. C., Allen, S. W., Craford, C. S., & Böhringer, H. 1997, *ApJ*, 479, L101
 Edge, A. C., Stewart, G. C., Fabian, A. C., & Arnaud, K. A. 1990, *MNRAS*, 245, 559
 Eke, V. R., Cole, S., & Frenk, C. S. 1996, *MNRAS*, 282, 263
 Fabian, A. C. 1994, *ARA&A*, 32, 277
 Gioia, I. M., Henry, J. P., Maccacaro, T., Morris, S. L., Stocke, J. T., & Wolter, A. 1990a, *ApJ*, 356, L35
 Gioia, I. M., Maccacaro, T., Schild, R. E., Wolter, A., Stocke, J. T., Morris, S. L., & Henry, J. P. 1990b, *ApJS*, 72, 567
 Henry, J. P., Gioia, I. M., Maccacaro, T., Morris, S. L., Stocke, J. T., & Wolter, A. 1992, *ApJ*, 386, 408
 Jones, C. J. & Forman, W. R. 1984, *ApJ*, 276, 38
 Jones, C. J. & Forman, W. R. 1998, *ApJ*, submitted
 Jones, L. R., Scharf, C. A., Ebeling, H., Perlman, E., Wegner, G., Malkan, M., & Horner, D. 1998, *ApJ*, 495, 100
 Kaiser, N. 1986, *MNRAS*, 222, 323
 Nichol, R. C., Holden, B. P., Romer, A. K., Ulmer, M. P., Burke, D. J., & Collins C. A. 1997, *ApJ*, 481, 644
 Rosati, P., Della Ceca, R., Norman, C., & Giacconi, R. 1998, *ApJ*, 492, L21

Stoche, J. T., Morris, S. L., Gioia, I. M., Maccaro, T., Schild, R., Wolter, A.,
Fleming, T. A., & Henry, J. P. 1991, *ApJS*, 76, 813

van Haarlem, M. P., Frenk, C. S., & White, S. D. M. 1997, *MNRAS*, 287, 817
Vikhlinin, A., McNamara, B. R., Forman, W., Jones, C., Quintana, H. &
Hornstrup, A. 1998, *ApJ*, in press (astro-ph/9803099)
White, S. D. M. & Rees, M. J. 1978, *MNRAS*, 183, 341